

PSHA input model documentation for Philippines (PHL)

GEM Hazard Team

Version history

Table 1 summarises version history for the PHL input model, named according to the versioning system described here, and indicating which version was used in each of the global maps produced since 2018. Refer to the GEM Products Page for information on which model versions are available for various use cases. The changelog describes the changes between consecutive versions and are additive for all versions with the same model year.

The following text describes v2018.3.0.

Table 1 *– Version history for the PHL input model.*

Version	2018.1	2019.1	2022.1	2023.1	2026.1	Changelog
v2018.0.0	X					First version of the model created under the PHIVOLCS-GEM collaboration.
v2018.1.0						A catalogue provided by PHIVOLCS was merged with the ISC-GEM catalogue. Seismicity was reclassified. The largest crustal source zone from v2018.0.0 was divided into three zones and all sources were recalibrated. Several new subduction interface sources were added. Crustal faults were adjusted so that continuous fault traces were linked together into a single fault, and MFDs for faults with Mmax>7 were changed from GR to YC1985.
v2018.1.1						Fault sources were regenerated after a bug fix in the OQ-MBTK.
v2018.1.2		X	X			Interface sources that use hybrid MFDs were regenerated after a bug fix in the workflow, resulting in lower Mmax for each interface segment.
v2018.2.0				X		Mmin extended to M4 for crustal distributed seismicity. Source ids were revised to work with disaggregation by source. Inslab source files were consolidated into a single one. gmmLT.xml updated with more recent GMPEs.
v2018.3.0					X	The gmmLT was updated based on more recent analyses. Padding sources from OPA and SEA were added to improve model coverage near perimeters.

Authors: PHIVOLCS, K. Johnson, R. Styron

1 Summary

The model covering the Philippines was developed jointly by the Philippine Institute of Volcanology and Seismology (PHIVOLCS) and the Global Earthquake Model (GEM) in the OpenQuake (OQ) engine format.

The model is documented in more detail in:

Peñarubia, H.C., Johnson, K.L., Styron, R.H., Bacolcol, T.C., Sevilla, W.I.G., Perez, J.S., Bonita, J.D., Narag, I.C., Solidum Jr, R.U., Pagani, M.M. and Allen, T.I., 2020. Probabilistic seismic hazard analysis model for the Philippines. Earthquake Spectra, p.8755293019900521

The 2026 version of this model (v2018.3.0) also includes some sources from the models for South East Asia (SEA) and the Pacific ocean (OPA) to extend the coverage of the model.

2 Tectonic overview

The Philippines sits in one of the world's most tectonically active locations, with the subduction of several oceanic plates beneath the crust of the islands, and a very rapidly-slipping and distributed fault system running throughout the islands. The eastern margin of the archipelago contains the East Luzon and Philippines Trenches, where the Philippine Sea Plate subducts obliquely underneath the islands. The western edge of the major islands is an active margin where the Sunda plate subducts at the Manila and Negros trenches; in between these, the buoyant Palawan block resists subduction and forces E-W contraction farther east. Subduction continues around the southern island of Mindanao with many short trenches such as the Cotobato and Halmahera, though relative plate velocities seem to be low and these features are poorly understood. The obliquity of convergence between the bounding Sunda and Philippine Sea plates results in a major strike-slip fault system bisecting the islands, the left-lateral Philippine Fault System. This system has net slip rates of almost 30 mm/yr, rivaling continental plate boundary transforms such as the Alpine and San Andreas faults. In places, this system has transtensional or transpressional bends or jogs, causing more distributed deformation. Additional, smaller faults are distributed throughout the archipelago, such as reverse faults in the Visayas and normal to strike-slip faults in southern Luzon; many of these are capable of generating high magnitude 7 earthquakes, which can (and have been) very damaging to proximal population centers.

3 Basic Datasets

3.1 Earthquake Catalogues

We used the ISC-GEM extended catalogue (Weatherill et al. (2016)) clipped to the Philippines region (bounds of ~112.5-134°E and 1°S-24°N) and the PHIVOLCS catalogue, which was developed as part of the Philippine Earthquake Model PSHA Database(Bautista and Oike, 2000). The final catalogue has ~ 37,000 earthquakes $M_w \geq$2.82 from 1905-2014.

We also use Global Centroid Moment Tensor (GCMT) focal mechanisms from 1976-2015 (*Dziewonski et al., 1981; Ekström et al., 2012*).

3.2 Fault Database

A database of 115 crustal faults was compiled based on decades of investigation by PHIVOLCS. These faults have been integrated into the GEM Active Faults Database.

4 Hazard Model

4.1 Seismic Source Characterisation

The source model includes varying source typologies for the different tectonic settings. These include:

- Interface seisimicity with $M_w \geq$5.5 modeled as **complex faults**
- Instraslab seismicity in each subduction zone as well as the Halmahera slab, with $M_w \geq$6.5 modeled as **nonparametric ruptures**
- Active shallow crustal faults producing earthquakes $M_w \geq$6.5 modeled as **simple faults**
- Distributed active shallow seismicity modeled as a grid of **point sources**

The interface and intraslab geometries are built using the GEM Subduction Toolkit (Pagani et al., 2020). Surfaces are cut at 50 km depth to separate the shallower interface from the deeper slab top.

The occurrence rates were determined using the following methodologies, which vary by source typology. For rates derived from seismicity, we use subcatalogues classified to the respective tectonic settings, declustered using *Uhrhammer (1985)* windowing and filtered for completeness.

Interface We model subduction interfaces for the Manila, Philippines, Cotobato, East Luzon, Negros, and Sulu trenches. We divide the trenches and slabs into segments using boundaries defined by the seafloor bathymetry, seismicity patterns, convergence rate changes, and any other information available within the literature as follows:

- *Manila*: three segments based on a coupling model by *Hsu et al. (2012)* and a north-to-south decrease in convergence rates, with boundares at ~14° N, where the trench axis bends by ~45°, and ~16.5° N at the Scarborough Seamount and a sediment thickness contrast thought to affect subduction mechanics (*Hsu et al., 2012*)
- *Philippine*: two segments separated at ~5° N, where the Halmahera slab and Philippine slab begin to interact
- *East Luzon*: two segments separated by a drastic change in strike at ~15.5° N

The Cotobato, Sulu, and Negros trenches are unsegmented.

For the Manila, East Luzon, Philippine, and Cotabato trenches, we derive a magnitude-frequency distribution (MFD) for each interface segment using the hybrid approach of Pagani et al. (2020), which combines statistics from observed seismicity with a characteristic component derived from tectonics. The Sulu and Negros trenches use Gutenberg-Richter MFDs derived from seismicity rates. Source characteristics with references are summarized in Table 2. The listed characteristic magnitude (M_{char}) is the median magnitude computed from the scaling relationship *Thingbaijam and Mai (2017)*.

Trench segments are numbered with increasing distance along strike following the right-hand rule.

Sub. zone	**Seg.**	***a*-Value**	***b*-Value**	$M_{max,obs}$	M_{char}	**C (mm/yr)**	**Coupling**
Manila	1	4.083	0.835	7.63	7.89	90	0.01
	2	4.279	0.873	7.24	8.15	60	0.01
	3	6.195	1.108	7.33	8.49	50	0.01
Philippine	1	6.176	1.073	7.52	8.63	30	0.27
	2	4.689	0.927	7.41	8.04	30	0.27
Cotobato	1	3.318	0.678	8.30	8.08	35	0.41
East Luzon	1	3.546	0.770	7.60	8128	15	1.0
	2	8.308	1.724	6.40	8.14	9	0.02
Sulu	1	3.312	0.797	7.50	N/A	N/A	N/A
Negros	1	5.127	1.084	6.63	N/A	N/A	N/A

Table 2 *– Source parameters for subduction interfaces.* ***C****: convergence rate. Convergence rates are from Hsu et al. (2012) for the Manila trench, Rangin et al. (2016) and Galanga et al. (2007) for the East Luzon, Cotabato and Philippine Trenches. Coupling coefficients for the Cotabato trench are from Rangin et al. (2016), and from Galgana et al. (2007) for all others. See also Table 3 in Peñarubia et al. (2020)*

Intraslab In the seismic source model, segmentation boundaries from the interface extend into the slab, and are not meant to suggest barrier to rupture within the downgoing slab volume, but instead to allow spatial variability in observed seimsicity while still using non-parametric ruptures. We model the rupture geometries and rates following the standard

GEM methodology for slab earthquakes, described here. Results are in Table 3.

An intraslab source model is included for all segments of the Manila, Philippine, and Cotabato trenches. Additionally, we include the Halmahera slab - which is fully subducted and and dips in both directions - modelled in two segments separated by the hinge axis.

Subduction zone	**Segment**	***a*-Value**	***b*-Value**	$M_{max,obs}$
Manila	1	6.658	1.277	6.69
	2	2.999	0.691	6.85
	3	5.087	1.050	6.90
Philippine	1	6.176	1.073	7.52
	2	5.118	1.014	7.01
Cotabato	1	4.081	0.943	6.45
Halmahera	1	7.140	1.179	8.01
	2	8.219	1.429	7.60

Table 3 *– Source parameters for subduction intraslab sources. See also Table 3 of Peñarubia et al. (2020).*

Crustal faults The crustal faults are modelled from each fault's geometry, kinematics, and slip rate (parameters included in the GEM Active Faults Database) using the standard practice of the GEM Secretariat (Appendix **??**). For most faults, we assigneed a fixed lower seismogenic depth of 20 km, minimum magnitude of *MW*6.5, and aseismic coefficient of 0.3. The exception is sections of the Philippines fault system on Leyte Island, which are shown to be mostly creeping; these faults were given an aseismic coefficient of 0.9.

The final MFDs are double-truncated Gutenberg-Richter distributions, except those with $M_{max} \geq$7.0, which have Youngs and Coppersmith (1985) MFDs. The *b*-value is set to that of the encompassing source zone described in the next section (*Distributed seismicity*).

Distributed seismicity We model distributed seismicity with an approach that combines area sources with smoothed seismicity, incorporating methods from *Frankel (1995)*, with the source zone approach commonly used to build GEM models; see Appendix F.2. We build a source model for the crustal subcatalogue encompassed by each source zone polygon, with occurrence rates at a bin spacing of *M*=0.1. We compute the smoothed seismicity for a grid of 0.1° spacing. The MFDs for grid points near faults are truncated at *MW*6.5 to prevent double counting (see *Crustal Faults* description). Source zone characteristics are described in Table 4.

4.2 Ground Motion Characterisation

The ground motion model has been updated for the 2026 release. Note that GMMs for sources originally from South East Asia (SEA) and the Pacific ocean model (OPA) are also shown.

Source zone	*a*-Value (zonal)	*b*-Value	$M_{max,obs}$	Description
0	5.619	0.959	7.75	shallow thrust faulting above the Halamahera slab
1	4.059	0.796	7.76	normal faulting, Philippine Trench outer rise
2	5.135	1.019	7.60	normal faulting, Manila, Sulu, and Negros Trench outer rises
3	3.779	0.814	7.15	diffuse crustal seismicity
4	4.998	0.904	7.80	reverse and left-lateral crustal faulting within southwest archipelago
5	3.205	0.620	7.69	fore- and backarc thrusting, overriding plate of Philippine trench
6	5.826	1.003	8.00	High-rate shallow deformation, includes PFS
7	5.191	1.098	7.30	normal faulting along the fore-arc of the Manila Trench

Table 4 *– Crustal source zone descriptions. PFS: Philippine Fault System. See also Table 1 of Peñarubia et al. (2020)*

Active Shallow Crust	**Weight**
BooreEtAl2014LowQ	0.25
CampbellBozorgnia2014	0.25
ChiouYoungs2014	0.25
BooreEtAl2014	0.25
Subduction Interface	**Weight**
AbrahamsonGulerce2020SInter	0.25
ParkerEtAl2020SInter	0.25
KuehnEtAl2020SInter	0.25
AbrahamsonEtAl2015SInter	0.25
Subduction IntraSlab	**Weight**
AbrahamsonGulerce2020SSlab	0.25
ParkerEtAl2020SSlab	0.25
KuehnEtAl2020SSlab	0.25
AbrahamsonEtAl2015SSlab	0.25
Active Shallow Crust SEA	**Weight**
BooreEtAl2014	0.25
CampbellBozorgnia2014	0.25
ChiouYoungs2014	0.25
CauzziEtAl2014	0.25
Oceanic Crust with Volcanism	**Weight**
Atkinson2010Hawaii	0.20
AbrahamsonEtAl2014RegJPN	0.20
BooreEtAl2014	0.20
CampbellBozorgnia2014	0.20
ChiouYoungs2014Japan	0.20

Table 5 *– GMMs used in the PHL model.*

5 Results

Hazard curves were computed with the OQ engine for the following:

- Intensity measure types (IMTs): peak ground acceleration (PGA) and spectral acceleration (SA) at 0.1s, 0.2s, 0.3s, 0.6s, 1.0s, and 2s
- reference site conditions with shear wave velocity in the upper 30 meters (Vs30) of 760-800 m/s, as well as for Vs30 derived from a topography proxy (Allen and Wald, 2009)

Hazard maps were generated for each reference site condition-IMT pair for 10% and 2% probabilities of exceedance (POEs) in 50 yrs. Additionally, disaggregation by magnitude, distance, and epsilon was computed for the following cities: Manila. The results were produced as csv files and bar plots for each of the following combinations:

- hazard levels for 10% and 2% POE in 50 yrs
- PGA and SA at 0.1s, 0.2s, 0.3s, 0.6s, 1.0s and 2.0s
- Vs30=800 m/s

All calculations used a ground motion sigma truncation of 5. Onshore results were computed for sites with 6 km spacing.

Visit the GEM Interactive Viewer to explore the Global Seismic Hazard Map values (PGA for Vs30=800 m/s, 10% poe in 50 years). For a comprehensive set of hazard and risk results, see the GEM Products Page.

6 References

Allen, T. I., and Wald, D. J., 2009, On the use of high-resolution topographic data as a proxy for seismic site conditions $Vs30$, Bulletin of the Seismological Society of America, 99, no. 2A, 935-943

Hsu, Y. J., Yu, S. B., Song, T. R. A., & Bacolcol, T. (2012). Plate coupling along the Manila subduction zone between Taiwan and northern Luzon. Journal of Asian Earth Sciences, 51, 98-108.

Peñarubia, H.C., Johnson, K.L., Styron, R.H., Bacolcol, T.C., Sevilla, W.I.G., Perez, J.S., Bonita, J.D., Narag, I.C., Solidum Jr, R.U., Pagani, M.M. and Allen, T.I. (2020). Probabilistic seismic hazard analysis model for the Philippines. Earthquake Spectra, p.8755293019900521

Rangin, C. (2016). Rigid and non-rigid micro-plates: Philippines and Myanmar-Andaman case studies. Comptes Rendus Geoscience, 348(1), 33-41.

A GEM modelling methods

B Catalogues

Much of PSHA depends on the assumption that future seismicity will occur near observed past seismicity, and at rates that can be approximated by empirical or physical models. Thus, the early steps in PSHA include compiling and processing an earthquake catalogue. Beyond collecting instrumental and historic earthquake records, catalogues must be homogenized (expressed in uniform units), declustered (devoid of aftershocks and foreshocks), and filtered for completeness. The assumptions and uncertainties in the catalogue should be well understood by the modeler.

Most source types used in hazard models built by the GEM Secretariat use magnitude-frequency distributions (MFDs, Section C) based on seismicity. Together with ground motion prediction equations (GMPEs), MFDs govern the computed hazard levels for time frames of interest, and so their robust calculation - and thus careful preparation of the input catalogue - is critical.

Here, we describe the GEM global catalogue which contributes the majority of earthquakes used in hazard models built internally by GEM; the workflow for combining other earthquake records with the global catalogue; and the remaining steps to prepare the catalogue for rate and spatial analysis. We emphasize that while most of these steps are routinely applied outside of GEM models, the following explanations only account for our own best practices.

B.1 The GEM global catalogue

The GEM global catalogue us a homogensised catalogue combining three global catalogues: the ISCGEM catalogue (*International Seismological Centre, 2025; Storchak et al., 2013, 2015; Di Giacomo et al., 2018*), the Global CMT catalogue (*Dziewonski et al., 1981; Ekström et al., 2012*) and the comcat/ANSS (*USGS, 2017*) catalogue and includes events from 1900, homogenised to M_W. This catalogue is periodically updated with new releases of the ISCGEM catalogue and to include more recent events from GCMT and comcat.

Recent regional models developed by the GEM Secretariat use the GEM extended catalogue, augmented by data from local agencies when possible.

B.2 Processing of seismicity catalogues

B.3 Catalogue homogenization

In order to use the bulletins from multiple agencies together in statistical analyses, records must be homogenized to meet the same criteria, e.g., to use the same measure of magnitude. Usually, moment magnitude (*MW*) is selected, since it does not saturate at high magnitudes. Thus, magnitudes reported in other scales must be converted. When pos-

sible, this is done using empirical relations developed for independent local datasets, but relies on global relations when too few calibration events are available.

The homogenization methodology used to build the catalogues is described in detail in *Weatherill et al. (2016)*.

B.4 Completeness analysis

Catalogue completeness analysis accounts for the variability in instrumentation coverage throughout the catalogue duration, admitting that any catalogue is missing earthquakes beneath a magnitude threshold. This type of filtering prevents rate analysis of an incomplete catalogue - a modeling mistake that will propagate into hazard estimates. Importantly, completeness analysis must be applied to a declustered catalogue as to not confuse dependent earthquakes (such as aftershocks) with magnitude completeness.

The completeness algorithms that are applicable to *any* instrumental catalogue must depend on properties of the earthquakes, and not the stations, thus focusing on the statistics of the catalogue sample rather than the probability that a station at a known position would record an earthquake. The most common algorithmic method is by Stepp (1971), which compares the observed rate of seismicity to a predicted Poissonian rate for each magnitude, and returns a spatially constant table of time-variable magnitude thresholds. Importantly, the validity of this methodology is subject to the judgement of the user.

The Stepp (1971) is implemented in the OpenQuake Engine, and used in some steps of the modeling procedure for hazard models built by the GEM Secretariat. In other cases, we determine the completeness manually from 3D histograms that count earthquakes for magnitude-time bins, visually identifying the timings at which the occurrences rates stabilize. In recent models, we use a newly-developed approach that jointly estimates the completeness and recurrence parameters, implemented in the OQ Model Builder's toolkit (MBTK, Pagani et. al, 2026). This approach reflects the inter-dependence of these parameters.

B.5 Declustering

Catalogue declustering is applied in order to isolate mainshock earthquakes - that is, earthquakes that occur independently of each other - from a complete catalogue. The resulting declustered catalogue should therefore reflect the Poissonian rate at which earthquakes occur within a greater tectonic region. PSHA aims to model the hazard from sesimicity occurring at this background Poissonian rate.

Declustering algorithms identify mainshocks by comparing individual earthquakes to the "cluster" of earthquakes that occurred within a given proximity and time to that earthquake, choosing the largest for a given set of magnitude-dependent "triggering windows". The theory of declustering algorithms is described in detail in *Stiphout et. al., 2012*. The OpenQuake

Hazard Modeler's Toolkit provides three different windowing options: the original implementation of Gardner and Knopoff (1974), and additionally the configurations of Uhrhammer (1986) and Gruenthal (see Stiphout et al., 2012).

In subduction zones or other complex environments, we first classify the seismicity by tectonic domain (described below), and then decluster groups of domains within which we expect seismicity to interact (i.e., interface mainshocks can trigger crustal aftershocks), and then separate the deemed mainshocks into subcatalogues based on their tectonic classification. We typically use two groups: crustal, interface, and shallow slab seismicity (that beneath the interface but with intraslab mechanisms); and deep intraslab seismicity. The declustering algorithm comparing epicentral (*not* hypocentral) proximities, and thus, declustering by groups is crucial for seismicity within slab-type volumes.

B.6 Classification of seismicity

The workflow used by GEM to construct seismic source models in complex tectonic regions is dependent on the use of classified seismicity, that is, the assignment of each earthquake to a tectonic domain. Separating earthquakes in this manner allows us to compute MFDs from only the seismicity occurring within a delineated domain, thus more accurately characterizing individual seismic sources or source zones. For example, in subduction zones, we separate earthquakes occurring on the interface itself from those within the downgoing slab or the overriding plate. This allows us to model the hazard from these source types using the appropriate GMPEs.

At GEM, we classify seismicity using an procedure with similar theory to *Zhao et al., (2015)* and *Garcia et al., (2012)*, which assigns earthquakes to tectonic domains defined by the modeler. In subduction zones, earthquakes are usually categorized as crustal, interface, or intraslab based on hypocentral proximity to the Moho, and the interface and slab-top complex surfaces defined by the (Subduction Toolkit). Where subduction zones are modeled as segmented interfaces or slabs, the domains are divided accordingly. Each tectonic domain is defined by a surface and a buffer region based on general characteristics of the corresponding cross sections. The modeler provides a tectonic hierarchy that chooses among multiple assignments for earthquakes occurring within overlapping buffers of two or more domains. Usually, we specify interface superseding intraslab, and intraslab superseding crustal. Earthquakes that do not correspond to any of the defined domains are deemed "unclassified".

The classification routine includes workarounds to correct some common misclassifications, such as to seclude dominant groups of earthquakes beneath a polygon (e.g., volcanic events); to classify large magnitude earthquakes from historic catalogues only by epicenter; and the ability to manually classify earthquakes by their event IDs.

B.7 References

Albini P., Musson R.M.W., Rovida A., Locati M., Gomez Capera A.A., and Viganò D. (2014). The Global Earthquake History. Earthquake Spectra, May 2014, Vol.30, No.2, pp. 607-624. http://doi.org/10.1193/122013EQS297

Di Giacomo, D., E.R. Engdahl and D.A. Storchak (2018). The ISC-GEM Earthquake Catalogue (1904–2014): status after the Extension Project, Earth Syst. Sci. Data, 10, 1877-1899, doi: 10.5194/essd-10-1877-2018.

Dziewonski, A. M., T.-A. Chou and J. H. Woodhouse, Determination of earthquake source parameters from waveform data for studies of global and regional seismicity, J. Geophys. Res., 86, 2825-2852, 1981. doi:10.1029/JB086iB04p02825

Ekström, G., M. Nettles, and A. M. Dziewonski, The global CMT project 2004-2010: Centroid-moment tensors for 13,017 earthquakes, Phys. Earth Planet. Inter., 200-201, 1-9, 2012. doi:10.1016/j.pepi.2012.04.002

Gardner, J. K., and Leon Knopoff. "Is the sequence of earthquakes in Southern California, with aftershocks removed, Poissonian?." Bulletin of the Seismological Society of America64.5 (1974): 1363-1367.

Stepp, J. C. (1971). "An investigation of earthquake risk in the Puget Sound area by the use of the type I distribution of largest extreme". PhD thesis. Pennsylvania State University (cited on pages 9, 25–27).

Stiphout, T. van, J. Zhuang, and D. Marsan (2012). Theme V -Models and Techniques for Analysing Seismicity. Technical report. Community Online Resource for Statistical Seismicity Analysis. URL: http://www.corssa.org.

Storchak, D.A., D. Di Giacomo, I. Bondár, E.R. Engdahl, J. Harris, W.H.K. Lee, A. Villaseñor and P. Bormann (2013). Public Release of the ISC-GEM Global Instrumental Earthquake Catalogue (1900-2009). Seism. Res. Lett., 84, 5, 810-815, doi: 10.1785/0220130034.

Storchak, D.A., D. Di Giacomo, E.R. Engdahl, J. Harris, I. Bondár, W.H.K. Lee, P. Bormann and A. Villaseñor (2015). The ISC-GEM Global Instrumental Earthquake Catalogue (1900-2009): Introduction, Phys. Earth Planet. Int., 239, 48-63, doi: 10.1016/j.pepi.2014.06.009.

Uhrhammer, Robert A. "SEISMICITY RECORD, M> 2.5, FOR THE CENTRAL." Clement F. Shearer (1985): 199.

U.S. Geological Survey, Earthquake Hazards Program, 2017, Advanced National Seismic System (ANSS) Comprehensive Catalog of Earthquake Events and Products: Various, https://doi.org/10.5066/F7MS3QZH.

Weatherill, G. A., M. Pagani, and J. Garcia. "Exploring earthquake databases for the creation of magnitude-homogeneous catalogues: tools for application on a regional and global scale." Geophysical Journal International 206.3 (2016): 1652-1676.

C Types of MFDs

In probabilistic seismic hazard analysis (PSHA), source models require a defined occurrence rate for earthquakes of each considered magnitude, e.g., a magnitude-frequency distribution (MFD). These rates are determined either by statistically analysing the observed seismicity over instrumental and historic time scales, or-for well characterized sources—by using the fault dimensions and slip rates to model recurrence.

Regional models built by GEM use the following common approaches to characterize seismicity rates.

C.1 Gutenberg-Richter

The Gutenberg-Richter MFD allows earthquake sources to generate earthquakes of different magnitudes. *Gutenberg and Richter (1944)* were the first to develop a functional form for the relationship between earthquake magnitude and occurrence rate, resolving a negative exponential distribution:

$$logN = a - bm \tag{1}$$

(2)

where *N* is the annual rate of earthquakes with *M* > *m*, *a* is the rate of all earthquakes, and *b* is the relative distribution of earthquakes among magnitudes. A higher *b*-value indicates a larger proportion of seismic moment released by small earthquakes. *a* and *b* are resolved from the available observations. Usually, *b* is close to 1.0.

C.1.1 Truncated Gutenberg-Richter

A traditional Gutenberg-Richter MFD allows for earthquakes of any magnitude, but in reality, the source in question may not be capable of producing earthquakes beyond a certain threshold. For example, fault dimensions physically limit earthquake magnitude, or the observed earthquake magnitudes saturate. To account for these constraints, a truncated MFD is used to specify a maximum magnitude (*Mmax*), simply by cutting the MFD at this magnitude. The MFD is additionally cut at a minimum magnitude ("double-truncated"), below which earthquakes are not contributing to the hazard in ways significant to engineering.

Truncated Gutenberg-Richter MFDs are commonly used in hazard models build by the GEM Secretariat. Where MFDs are produced for a source zone, such as for distributed or inslab seismicity, the upper magnitude is usually determined by adding a delta value (e.g., *MW*0.5) to *Mmax* in the earthquake catalogue or subcatalogue used to produce the MFD. This is based on the premise that the observation period is too short to have experienced a true *Mmax* earthquake.

GEM models typically use the methodology of Weichert (1985) to compute double-truncated Gutenberg-Richter MFDs for seismic source zones, which allows for the use of different observation periods for different earthquake magnitudes (e.g., a completeness threshold).

If a seismicity distribution is not explicitly available, an MFD of this form can also be computed from a seismic moment budget using strain rates, fault dimensions, and assumed magnitude ranges and *b*-values. For models built internally by GEM, we apply this to faults with available slip rates.

C.2 Characteristic

Some sources do not produce earthquakes that follow the Gutenberg-Richter distribution, but instead tend to host earthquakes of nearly the same magnitude, e.g., a characteristic earthquake. In this case, an earthquake with a moderate to high magnitude occurs more frequently than would be suggested by a Gutenberg-Richter MFD. For sources of this type, the MFD reveals more frequent occurrences concentrated around the most-likely/characteristic magnitude earthquake, for example using a boxcar or Gaussian distribution (e.g., *Youngs and Coppersmith, 1985*, or *Lomnitz-Adler and Lomnitz, 1979*).

Though the *Youngs and Coppersmith* (*1985*) MFD is technically a hybrid MFD, incorporating both a characteristic component and a Gutenberg-Richter component at lower magnitudes, it is typically often categorized as a characteristic MFD. GEM uses this MFD in a few models built in-house, such as the Philippines model, where sensitivity testing indicated that it produced a better fit to the regional seismicity than a double-truncated GR for crustal faults.

C.3 Hybrid types

Some subduction interface source models built by the GEM secretariat use a hybrid approach that combines the Gutenberg-Richter MFD with a characteristic MFD. The latter approach derives a double truncated Gaussian distribution to model occurrence of the maximum magnitude (*M*max) earthquake that an interface segment can theoretically support (herein called the "characteristic earthquake").

The magnitude and occurrence rate of the characteristic earthquake for an interface segment are based on the fault area (e.g., from the complex fault output by the Subduction Toolkit), the convergence rate, and a seismic coupling coefficient. We choose between three recent scaling relationships for subduction interfaces that compute magnitude from fault area: *Strasser et al.* (*2010*), *Allen and Hayes* (*2017*), and *Thingbaijam and Mai* (*2017*). We use published convergence rates and seismic coupling coefficients to determine the time needed to accumulate enough strain for the characteristic earthquake. The coupling parameter is often challenging, in large part due to the scarcity of land and thus GPS measurements in close proximity to subduction zones. Where no other model is available, we take values from *Heuret et al.* (*2011*) or *Scholz and Campos* (*2012*), but cautiously, as many

sometimes these values are suspiciously low (e.g., <0.1 where instrumentally recorded earthquakes *M*>8.0 have occurred.)

The characteristic MFD is combined with the Gutenberg-Richter MFD into a hybrid MFD by finding the intersection point of the two MFDs, and taking the Gutenberg-Richter occurrence rate below the intersection magnitude, and the characteristic rate above that magnitude.

C.4 References

Allen, T. I., & Hayes, G. P. (2017). Alternative rupture-scaling relationships for subduction interface and other offshore environments. *Bulletin of the Seismological Society of America*, 107(3), 1240-1253.

Gutenberg, B., & Richter, C. F. (1944). Frequency of earthquakes in California. *Bulletin of the Seismological Society of America*, 34(4), 185-188.

Heuret, A., Lallemand, S., Funiciello, F., Piromallo, C., & Faccenna, C. (2011). Physical characteristics of subduction interface type seismogenic zones revisited. *Geochemistry, Geophysics, Geosystems*, 12(1).

Lomnitz-Adler, J., & Lomnitz, C. (1979). A modified form of the Gutenberg-Richter magnitude-frequency relation. *Bulletin of the Seismological Society of America*, 69(4), 1209-1214.

Scholz, C. H., & Campos, J. (2012). The seismic coupling of subduction zones revisited. Journal of Geophysical Research: *Solid Earth*, 117(B5).

Thingbaijam, K. K. S., Martin Mai, P., & Goda, K. (2017). New empirical earthquake source-scaling laws. *Bulletin of the Seismological Society of America*, 107(5), 2225-2246.

Strasser, F. O., Arango, M. C., & Bommer, J. J. (2010). Scaling of the source dimensions of interface and intraslab subduction-zone earthquakes with moment magnitude. *Seismological Research Letters*, 81(6), 941-950.

D Subduction modelling

Subduction zones are plate margins where one tectonic plate 'subducts' or is thrust beneath another plate. These zones produce most of the seismicity on Earth. The zones can be complex, producing earthquakes at the interface or 'megathrust' fault between the plates, in the downgoing plate or 'slab', and in the deforming region at the margin of the upper, overriding plate. For hazard models produced by the GEM Secretariat, the plate interface and the subducting slab are characterized and modeled with subduction-specific tools we have developed alongside our modeling efforts, while the deformation within the upper plate is modeled as part of the active shallow crust.

D.1 Subduction interface

Among PSHA models, various source model approaches are used to model interface seismicity. Models produced by GEM use OpenQuake complex faults (surfaces with complex geometry) to account for subduction interface seismicity, and float all possible ruptures within specified magnitude limits and have a given rupture aspect ratio across the meshed surface. In some cases, we segment the surfaces along-strike to define firm barriers to rupture or capture changes in subduction characteristics. We use two predominant approaches to compute magnitude-frequency distributions (MFDs) and maximum magnitudes of the interface segments. Both use recorded instrumental (and sometimes historical) seismicity that can be attributed to the respective interface segment (classified using the methodolgy described in Section B.6), fitting a Gutenberg-Richter (a negative exponential) distribution to the seismicity. One approach also includes a characteristic component, computed from the area of the interface surface, the local convergence rate, and the degree of seismic locking (a seismic coupling coefficient). MFD construction is explained in detail in Section C.

D.2 Slab

Hazard models built by the GEM Secretariat account for intraslab seismicity using nonparametric ruptures (sources with predefined geometry) that fit within a slab volume of uniform thickness. The ruptures correspond to virtual faults within a meshed approximation of the slab volume, and forces ruptures to fit within the slab. Like the interface, the slab volume can be segmented, however here, boundaries only seldom indicate barrier to rupture (such as at a slab tear) and are more commonly used to reflect change in seismicity rate. For each slab segment, we compute a single Gutenberg-Richter MFD from the slab segment subcatalogues produced during tectonic classification (Section B.6), assuming constant rates throughout each segment. Currently, moment rates are distributed uniformly among the computed ruptures, but future development will include a smoothing component.

E The Subduction Toolkit: building the geometry of the interface surface and slab volume

Alongside the PSHA models that incorporate subduction zones, GEM has developed the Subduction Toolkit, which uses an interactive workflow to build the subdction interface and slab top geometry, an integral step in producing the subduction source model.

The subduction geometries are based on trench axes from the GEM Active Faults Database along with several geophysical datasets and models. The toolkit projects swaths of geophysical data onto cross sections along a trench axis, which are used to guide depth picking for the interface and slab upper surface. These depth profiles are then stitched together to form OpenQuake complex fault surfaces, which are used as reference frames for catalogue tectonic classification (Section B.6), and for defining subduction source geometry (described above).

The data plotted on the cross sections is meant to illuminate the subsurface subduction structures and tectonic processes that contribute to seismic hazard (e.g., Figure 1). The most commonly used data include:

- hypocenters from ISC-GEM catalogue (*Weatherill et al., 2016*)
- centroid moment tensors (CMTs) from the Global CMT project (*Dziewonski et al., 1981*; *Ekstrom et al., 2012*)
- Moho depth estimates from Lithos1.0 (*Pasyanos et al., 2014*) and Crust1.0 (*Laske et al., 2013*)
- Slab depth estimates from Slab1.0 (*Hayes et al., 2011*) and Slab2.0 (*Hayes et al., 2018*)
- Shuttle Radar Topography Mission (SRTM) topography (*Farr, 2007*)
- General Bathymetric Charts of the Ocean (GEBCO) bathymetry (*Weatherall et al., 2015*)
- Volcano locations

Initially, the cross sections are automatically generated at a specified increment along the trench axis that balances data density with resolution, with azimuths perpendicular the trench. The cross section origins and azimuths can then be adjusted manually, and additional cross sections added where necessary.

The final depth profiles (or a subset) are stitched together to form an OpenQuake complex fault surface. The Toolkit allows for the full extent of the profiles to be considered in subsequent steps, or a depth range can be defined. We use these capability to separate the subduction interface from the deeper slab, and to segment the surfaces along strike (see above).

E.1 References

Dziewonski, A. M., T.-A. Chou and J. H. Woodhouse, Determination of earthquake source parameters from waveform data for studies of global and regional seismicity, J. Geophys. Res., 86, 2825-2852, 1981. doi:10.1029/JB086iB04p02825

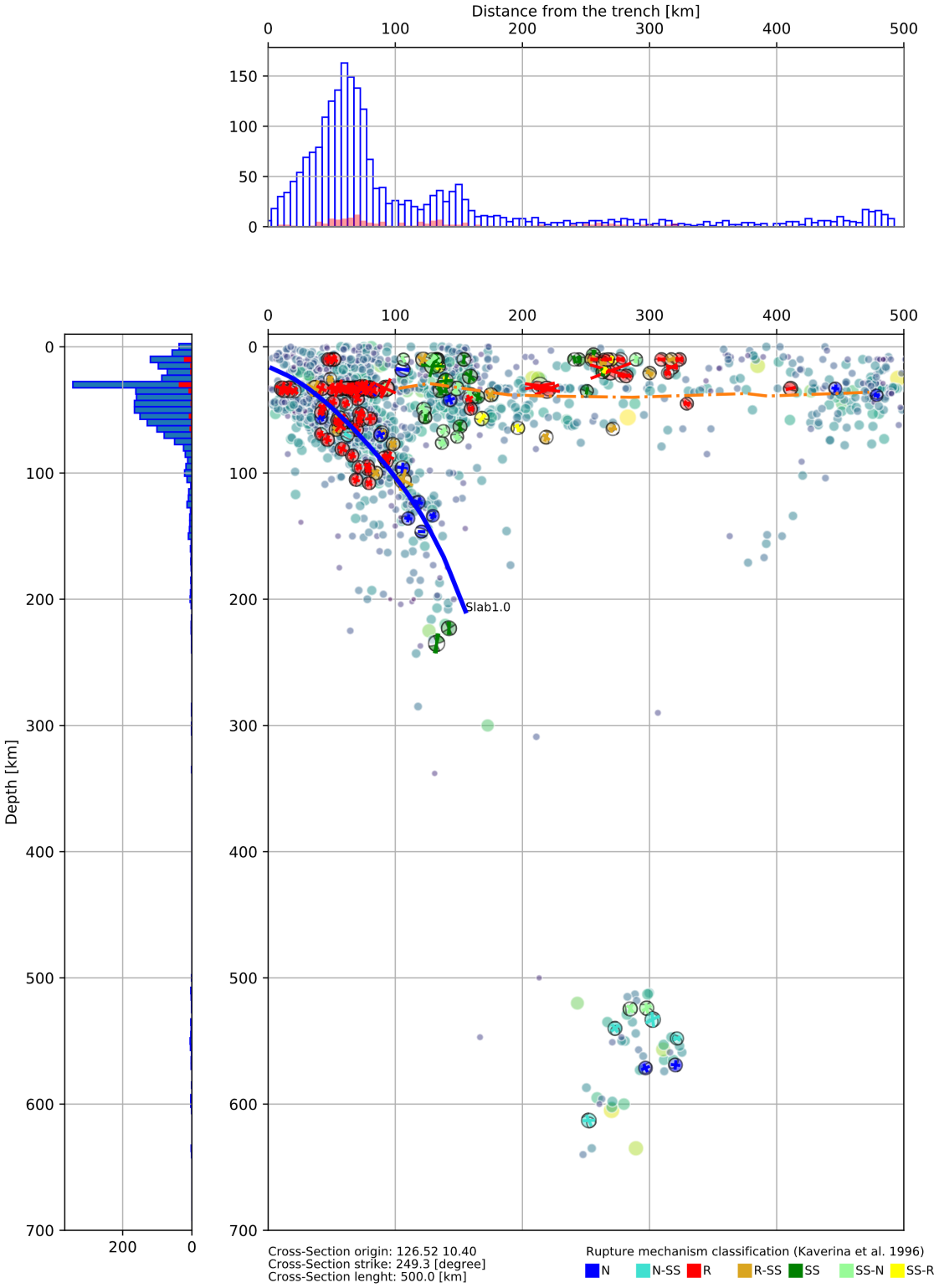


Figure 1 *– Example cross-section of a subduction zone from the Philippines*

Ekström, G., M. Nettles, and A. M. Dziewonski, The global CMT project 2004-2010: Centroid-moment tensors for 13,017 earthquakes, Phys. Earth Planet. Inter., 200-201, 1-9, 2012. doi:10.1016/j.pepi.2012.04.002

Farr, T.G., Rosen, P.A., Caro, E., Crippen, R., Duren, R., Hensley, S., Kobrick, M., Paller, M., Rodriguez, E., Roth, L. and Seal, D., 2007. The shuttle radar topography mission. Reviews of geophysics, 45(2), doi:10.1029/2005RG000183.

Hayes, Gavin P., David J. Wald, and Rebecca L. Johnson. "Slab1. 0: A three-dimensional model of global subduction zone geometries." Journal of Geophysical Research: Solid Earth 117.B1 (2012).

Hayes, G. P., Moore, G. L., Portner, D. E., Hearne, M., Flamme, H., Furtney, M., & Smoczyk, G. M. (2018). Slab2, a comprehensive subduction zone geometry model. Science, 362(6410), 58-61.

Laske, Gabi, et al. "Update on CRUST1. 0—A 1-degree global model of Earth's crust." Geophys. Res. Abstr. Vol. 15. Vienna, Austria: EGU General Assembly, 2013.

Pasyanos, Michael E., et al. "LITHO1. 0: An updated crust and lithospheric model of the Earth." Journal of Geophysical Research: Solid Earth 119.3 (2014): 2153-2173.

Weatherall, P., K. M. Marks, M. Jakobsson, T. Schmitt, S. Tani, J. E. Arndt, M. Rovere, D. Chayes, V. Ferrini, and R. Wigley (2015), A new digital bathymetric model of the world's oceans, Earth and Space Science, 2, 331–345, doi:10.1002/2015EA000107.

Weatherill, G. A., M. Pagani, and J. Garcia. "Exploring earthquake databases for the creation of magnitude-homogeneous catalogues: tools for application on a regional and global scale." Geophysical Journal International 206.3 (2016): 1652-1676.

F Modelling distributed seismicity

We use the term "distributed seismicity" to indicate earthquakes not clearly attributable to an individual fault source or subduction zone. To model these, we group together seismicity with common characteristics, such as focal mechanism type, strain by the same tectonic forces, rate, or 3D distribution; we then produce source models reflecting these characteristics. Here, we describe two primary source types used to model distributed seismicity.

F.1 Area Sources

Area sources consist of a statistically-determined MFD (Section C) from earthquakes occuring in a volume (usually a polygon, defined by the modeler, with depth limits), with the modelled occurrence rates distributed uniformly (equal *a*- and *b*-values) over an evenly spaced grid, and paired with a hypocenter and focal mechanism. In the OpenQuake Engine, the specified hypocentral depths and focal mechanisms can be probability distributions, or singular metrics.

F.2 Smoothed Seismicity

Smoothed seismicity is modeled similarly to area sources, but rather than using a spatially-homogeneous MFD in each source, the *a*-values vary spatially based on observed seismicity.

GEM has moved away from using traditional area sources, and predominantly models distributed seismicity with an approach that combines area sources with smoothed sesimicity, incorporating methods from Frankel (1995). We define a few source zones with internally consistent tectonics (e.g., up to a few prominent focal mechanism types, reflecting the same tectonic stresses), solve for the Gutenberg-Richter *b*-value, and then smooth the occurring seismicity onto a grid of points. This approach allows us to use larger source zones (and thus more earthquakes to compute a more robust MFDs) while still capturing spatial variability in seismicity rate.

We use the declustered crustal sub-catalogue, applying the *Stepp (1971)* completeness analysis or one based on time-magnitude density plots. Then, from the earthquakes within each source zone, we compute a double truncated Gutenberg-Richter MFD from M=5 to $M_{max,obs}$ + 0.5 (bins of M 0.1), solving for *a*- and *b*-values based on *Weichert (1980)*. We classify the earthquake probability into weighted depth bins. Lastly, we assign most-likely nodal planes based on crustal earthquake focal mechanisms within the source zone based on the GCMT catalogue.

We compute the smoothed seismicity grid by applying a Gaussian filter to the clipped, declustered catalogue for each source zone, and computing the fraction of spatial seismicity rates at each grid node. These are combined with the zone MFD to compute a grid of point-by-point earthquake occurrence rates.

In areas where we also model fault sources, we prevent double counting by dividing the magnitude occurrence bins between the two source types. If there is overlap (including a buffer around the surface projection of a fault, we cut the MFDs for distributed seismicity at *Mmax*=6.5, and use the same value as *Mmin* for fault MFDs.

F.3 References

Frankel, A. (1995). Mapping seismic hazard in the central and eastern United States. Seismological Research Letters, 66(4), 8-21.

Stepp, J. C. (1971). "An investigation of earthquake risk in the Puget Sound area by the use of the type I distribution of largest extreme". PhD thesis. Pennsylvania State University (cited on pages 9, 25–27).

Weichert, Dieter H. "Estimation of the earthquake recurrence parameters for unequal observation periods for different magnitudes." Bulletin of the Seismological Society of America70.4 (1980): 1337-1346.